Chapter 3

Antibacterial Activity of Metallic Nanoparticles

Shamaila Shahzadi, Nosheen Zafar and
Rehana Sharif

Additional information is available at the end of the chapter

http://dx.doi.org/10.5772/intechopen.72526

Abstract

Metallic nanoparticles (NPs) for medical applications have been documented since earlier times. Advancement in modern medicines results in an increase in utilization of NPs for medical purposes due to their antibacterial, antiviral, antifungal, anti-inflammatory, and antiangiogenic properties. In this chapter, three metallic NPs are studied extensively as powerful nanoweapons for the destruction of bacteria. Recent research gives evidence that metallic NPs are very effective in supporting antimicrobial activities. The chemically and laser-ablated silver, gold, and copper NPs exhibited enhanced antibacterial activity than previously reported. The antibacterial mechanism was found dose- and size-dependent and was more profound for Gram-negative bacterium as compared to Gram-positive ones. The dose calculations of minimum inhibitory concentration (MIC) with NPs have been calculated for both Gram-positive and Gram-negative bacteria. The maximum zone of inhibition by disk diffusion was also experimented against various bacteria. These NPs exhibit excellent performance physically, catalytically, and chemically. Present study will be beneficial in areas of environment, information technology, health, cosmetics, and food department. This chapter will cover the details of fabrication and antibacterial activity results of silver, gold, and copper NPs. This chapter endeavors to demonstrate the use of metallic NPs as an alternative antibacterial nanobiotics.

Keywords: laser ablation synthesis, wet chemical technique, antibacterial mechanism, Gram-positive bacteria, Gram-negative bacteria

1. Introduction

Recently, metallic nanomaterials have become the most enormous and rapid emerging materials of science areas. The increased attention of nanomaterial fabrication, especially nanoparticles (NPs), is due to their fascinating properties revealed by their size, high surface area, and extraordinary surface activity exhibiting outstanding catalytic, electrical, and optical properties. Thus, metallic NPs have participated in extensive applications of research methodology

and in advance micro- and nanotechnologies. They are proved as excellent heterogeneous catalysis, used in thin-film fabrication technology, in electronics, and in the manufacturing of microelectronic devices [1]. For controlled synthesis of NPs, the traditional colloid techniques are shared with modern techniques for [1]. Metallic NPs have powerful absorption spectrum in visible range, which is due to electron coherent oscillations on the surface of particles, called surface plasmon resonance (SPR). The SPR spectrum of metallic NPs has multiple applications in the field of biotechnology and has drawn enormous attraction recently [2, 3].

Silver is one of the widely studied metals during the last decades in nanotechnology research. Its distribution of size, stability, morphology, and surface charge/modification each plays a vital role in many scientific fields [1]. Its main features provide improvement in photography, microelectronics, photonics, photocatalysis, lithography, and antimicrobial and antifungal activity [4–6].

Gold (Au) NPs are also famous candidates for medical therapy, cancer treatment, gene therapy, diagnostics, drug delivery, and biological purposes [7–9]. Its main advantage is its simple formation by chemical reduction and exhibiting low toxicity. To improve the capability of gold NPs, different techniques have been employed that provide various dimensions of NPs and its functionalization [10–12]. Due to inert characteristics of gold NPs, it is well known for biocompatibility, but its cytotoxicity mostly depends on nanoparticle's size having precise concentration [13].

The next prominent metal is copper (Cu) that has similar optical, electrical, and thermal characteristics like silver and gold. The only disadvantage is its oxidation state during the synthesis process; thus, it is the major challenge for any scientist. Although gold is costly as compared to silver and copper, consequently the fabrication of the latter NPs develops into more complimentary in recent research [14]. Copper NPs provide an ideal compromise between its novel properties and cost, thus proving an important material for industry. In fact, its vast field of applications is magnetic media for storage devices, solar energy transformations, electronics, and catalysis, and in addition, it has revealed a promising antimicrobial action [15].

1.1. Synthesis methods for metallic NPs

Fabrication of metallic NPs can be achieved by three ways: (i) physical methods in which metallic aggregates subdivided mechanically such as by laser ablation, vapor deposition, wire discharge, and mechanical milling; (ii) chemical methods in which metallic atoms produce nucleation and then growth occurs; and (iii) biological methods in which metallic NPs are formed by the reduction of metallic salts with any plant serum. The physical techniques yield dispersions with broad distribution of particle size. Chemical methods such as salt reduction are convenient method for the controlled sized particles [16].

1.1.1. Laser ablation in liquid (LAL)

One of the advance and toxic-free techniques for nanoparticle fabrication is laser-ablated solid metal targets. In this technique, bulk target is positioned in any liquid environment and ablated by a pulsed laser. From ablated portion of the target, a dense plume of vapor and atomic clusters is ejected into the liquid environment and, thus, has rapid formation of NPs. This technology generates small, surfactant-free, and monodisperse NPs, having many advantages on chemical reduction technique [17–19] due to the use of toxic reducing agents. The size, dispersion, and composition of NPs generated by LAL method dispersed in liquid

medium can be well controlled [20–22] by adjusting the target, liquid type, and laser parameters, like wavelength, fluence, and pulse duration [23].

1.1.2. Wet chemical method for nanoparticle production

The second traditional method is wet chemistry mostly utilized to fabricate metallic NPs. This technique also has the ability to produce NPs of controlled morphology, composition, and crystallinity. Here, chemical reduction of salts generates comparatively larger NPs as compared to that of LAL technique [24, 25]. In wet chemical method, the formation of NPs has undergone by the following processes:

(A) Nucleation: The main process of synthesis initiates with the process of nucleation, in which a new phase particle called "seed" has been formed in a previous system of single phase (a homogenous solution of salt) [26]. With the additional attachment of metal atoms to this seed from solution, further growth of NPs is done. The shape of the NPs and its growth depends on the varying conditions of reaction [27–31].

(B) Seeding process: During the reduction process of salt, the metallic atom concentration enhances with the decomposition of precursor till a supersaturated state has been reached [32]. At this stage, the atoms begin to agglomerate and form nuclei of precise dimension called seed which further grow into crystallite [32]. Typically, precursors are metallic salts, mostly used as reducing agents [25, 32]. Capping agents are used to stabilize the metallic seed by preventing agglomeration and maintaining the nuclei size [33]. Seed-mediated nuclei growth process is one of the most efficient and effective processes because of low activation energy requirement for metal reduction process on to the preformed seeds to get NPs of controlled size and shape [34, 35].

(C) Nanoparticle formation: The nanoparticles are formed by the controlled competition of surface energy enhancement and a bulk energy diminution. An enhancement in the surface energy helps in dissolution, while decrease in bulk energy favors the process of growth [32]. Continued addition of atoms allows the seed to increase in size in a uniform manner. Thus, solutions of suitable metallic precursor, reducing agent and capping agent, are the basic necessity for the formation of metallic nanoparticles via chemical reduction method.

1.2. Antimicrobial mechanism of metallic NPs

Metal and metallic salts are well known for antibacterial mechanism for centuries as silver pots were used for drinking water from 4000 BCE [36, 37]. Recent research in nanophysics capable the scientist to study the antibacterial properties on various metallic NPs [38, 39].

Basic toxic antibacterial mechanism of metallic NPs is still under debate, but three main mechanisms are supposed which include, firstly, the formation of reactive oxidative species (ROS); secondly, releasing process of ions; and, finally, interaction of NPs with the cell membrane (**Figure 1**). Metallic NPs as compared to their salts have enhanced potential to combat bacterial infections [40–43]. Mostly, the size of NPs influences the antibacterial mechanism [44–49].

1.2.1. Entering the cell

The first step of antibacterial mechanism is the metallic ions of nanometer range attached to the cell via transmembrane protein. After attaching to bacterial cells, producing structural

changes in the cell membrane and blocking the transport channels [6, 50], the whole process is size dependent. Small NPs are more efficient, while larger NPs have a higher absolute surface area permitting for better adhesion property of van der Waals forces. Then, NPs may be internalized, produce ionization within the cell, and damage intracellular structures resulting in cell death (**Figure 1**) [40].

1.2.2. Reactive oxidative species (ROS) generation

The production of reactive oxidative species (ROS) by metal NPs plays a large role in their antibacterial effectiveness (**Figure 1**). ROS consist of short-lived oxidants, such as superoxide radicals (O^{-2}), hydrogen peroxide (H_2O_2), hydroxyl radicals (OH^{-1}), and singlet oxygen (O^{-2}) [51, 52]. Due to the high reactivity of these species, ROS can cause damage to peptidoglycan and cell membranes, DNA, mRNA, ribosomes, and proteins [42]. ROS can also inhibit transcription, translation, enzymatic activity, and the electron transport chain [42, 51]. Some metal oxide NPs rely on the generation of ROS as a main mechanism of toxicity [6, 41, 50].

1.2.3. Protein inactivation and DNA destruction

Metal atoms have the tendency to attach with thiol group of enzymes and finally deactivate the function of enzymes. It is also suggested that metal ions attach themselves between the pyrimidine and purine base pairs disturbing the bonding of hydrogen between two strands of antiparallel and destruct the molecule of DNA (**Figure 1**). Although this has to be further investigated, but this is true that metal ions have tendency to attach with DNA, once they go into the cell [53].

1.3. Detection methods

There are various direct and indirect methods for the microbial growth measurement. In direct method, mostly microbial effects are evaluated by viable technique of plate count, serial dilution,

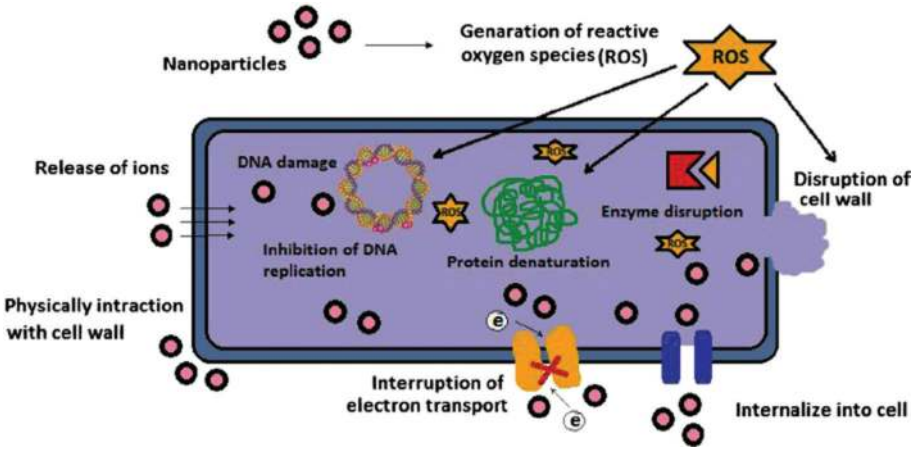

Figure 1. Various mechanisms of antimicrobial activity of the metal NPs [40].

and disk diffusion method, while indirect methods are analyzed by turbidity, dry weight, and by metabolic activity. In brief, short description of direct and indirect methods is as follows.

1.3.1. Viable plate count method

In the plate count techniques, Petri dishes are used for each reading. Agar plate is prepared, and one plate of inoculums and other plates with inoculum and nanoparticle solutions are spread on it with the help of sterile spreader; this plate is incubated for 24 hours at 37°C and then counted the colonies of each plate. Then, the inhibition percentage growth with each reading is calculated [54, 55].

1.3.2. Disk diffusion method

The prepared culture of bacteria is mixed in nutrient broth to form liquid culture. Then, sterile nutrient agar solution is prepared and put into dishes and waited to be solidified. After that, holes are generated with the help of cork borer. Bacterial culture is spread on the agar with sterile cotton bud. Holes are filled with solution of metallic NPs and stabilized; after that, the plates are incubated for 24 hours at 37°C. The zones of inhibition are observed the next day and calculated with standard error. For accurate analysis, proper repetition of the experiments is done for microbial study [16].

1.3.3. Estimating bacterial numbers by indirect methods

Indirect methods are basically referred as time-consuming methods, and the large number of samples is prepared at a time. A spectrophotometer is utilized to analyze the turbidity process by measuring the quantity of light that transmits through a bacterial cell suspension. As more transmission occurs through suspension, it means that turbidity decreases, indicating the reduction in bacterial cells and vice versa [56, 57].

2. Antibacterial mechanism of metallic nanoparticles

2.1. Antibacterial mechanism of silver nanoparticles (SNPs)

In recent research, Zafar et.al. [57] have worked on the antibacterial mechanism of silver NPs fabricated by laser ablation and by chemical method having different sizes and examined these NPs against Gram-positive (+) bacteria (*Bacillus subtilis* and *Staphylococcus aureus)* and Gram-negative (−) bacteria *(Salmonella*, *Escherichia coli*, and *Klebsiella pneumonia)* by turbidity method and by well diffusion method.

2.1.1. Turbidity method

A medium (nutrient broth) (5.00 ml) was arranged in the labeled tubes and then sterilized, thus forming broth media in transparent form. The bacterium culture was then ready by shifting an identified Gram-positive [*S. aureus* and *B. subtilis*] and Gram-negative bacteria's culture

[*Salmonella* and *E. coli*] into four (4) tubes of liquid nutrient broth with platinum wire. After the process of inoculation, tubes were incubated at 37°C for 1 day. The next day, a visible growth was observed in the tubes of culture. Then, these tubes of bacterium culture were strictly checked by various identification tests. Already measured doses (low, medium, and high) of sterilized SNPs were tested against this bacterium growth. Each tube had facilitated with medium (5 ml), inoculums (200 μl), plus the measured dose of SNP stock solution. Three tubes were arranged for each reading. Negative control tube had broth and NPs only, and positive control tube had broth and inoculums only. All tubes were incubated at 37°C for 24 hours.

Turbidity of tubes was confirmed by Elisa reader, a spectrophotometer having a filter of 600 nm wavelength. The values of optical density (OD) from Elisa reader in absorption mode represented the bacterial growth of labeled samples. Three OD values of each dose were taken, and their mean was calculated with standard deviation (St. Dev.). Three designed doses of SNPs were taken. Bacterial growth in nutrient broth revealed the total percentage (%) of bacterium growth. The percentage (%) change in the growth of bacterium was measured against OD value of pure nutrient media of broth (reference OD value). Similarly, the maximum calculated growth of *S. aureus*, *B. Subtilis*, *Salmonella*, and *E. coli* was 75.19, 68.5, 74.3, and 71.9%, respectively [57]. Contaminant in microorganism's growth was only 1.5% which is ignorable against growth of bacterium (**Table 1**).

Same process had been applied for the calculation of all doses. The growth of bacteria decreases with increasing dose of NPs [57]. Chemically synthesized SNPs inhibited 67.02% *S. aureus*, whereas *E. coli* was inhibited up to 87.9%. It indicated that more doses should design for full inhibition of *S. aureus*. *B. subtilis* was inhibited 39.9%, and *Salmonella* was inhibited only 80.2%. Laser-ablated SNPs inhibited the bacterium with higher efficiency having low dose (2.10 μg/ml). For example, 67.02% growth calculated with dose (2.35 μg/ml) for *S. aureus* diminished up to 92.0% with dose (2.10 μg/ml), whereas no growth appeared for *E. coli* with designed high doses. Similarly, the calculated growth of *Salmonella* is 18.0% that shows that the growth is reduced up to 82% [57].

Two sized SNPs were considered for antibacterial evaluation. The chemically synthesized SNPs have size range ~30–40 nm (Sample S1), while the laser-ablated SNPs had size range ~20–30 nm (Sample S2). Equal doses of laser-ablated NPs provided enhanced inhibition against each bacterium. Chemically synthesized SNPs exhibit less efficiency with respect to laser ablated SNPs. The first reason was slightly larger-sized nanoparticles, and, secondly, it might be possible that some chemical species may be adsorbed on the surface of NPs which declined the antibacterial

Inoculum	**OD value of culture (S)**	**OD value for culture** **R=S – 0.065±0.001**	**Percentage growth** $=\frac{R}{S} \times 100$ **(%St. Dev)**
S. aureus	0.262 ± 0.004	0.197 ± 0.005	75.19 ± 0.9
E. coli	0.253 ± 0.003	0.188 ± 0.004	74.3 ± 0.7
B. subtilis	0.207 ± 0.001	0.142 ± 0.002	68.5 ± 0.3
Salmonella	0.232 ± 0.001	0.167 ± 0.002	72 ± 0.3

Table 1. Percentage growth of *S. aureus*, *E. coli*, *B. subtilis*, and *Salmonella* observed in broth medium [57].

performance. Hence, for the pureness of sample, chemical fabrication has many restrictions to employ these NPs for the biological, catalytic, and sensing applications.

For statistical analysis and regression line, along X-axis, dose of SNPs was taken, whereas along Y-axis, percentage growth was plotted. Regression line has been plotted by using the values from **Table 2** in given equations:

$$b = \frac{\sum XY - \frac{\sum X \sum Y}{N}}{\sum X^2 - \frac{(\sum X)^2}{N}} \quad (1)$$

$$a = \frac{\sum Y}{N} - b\frac{\sum X}{N} \quad (2)$$

$$Y = a + bX \quad (3)$$

From regression lines (**Figure 2**), the calculated minimum inhibitory concentration (MIC) of chemically synthesized NPs (30–40 nm) was estimated as ~2.8, 13.5, 4.37, and 2.81 μg/ml for *E. coli*, *B. subtilis*, *S. aureus*, and *Salmonella*, respectively, whereas the calculated MIC for laser-ablated NPs (20–30 nm) were ~2.10, 2.68, and 2.36 μg/ml for *E. coli*, *Salmonella*, and *S. aureus*, respectively. Student's t-test with $p < 0.05$ was applied to all experimental data.

2.1.2. Well diffusion method for silver nanoparticles

Antibacterial mechanism was further evaluated against *S. aureus* and *E. coli* with same doses of SNPs by well diffusion method [57]. The results [57] obviously determined the zone of inhibition for laser-ablated and chemically synthesized SNPs, and no zone appeared in the control. Further, the inhibition zones due to laser-ablated NPs are considerably enhanced as compared to chemically synthesized SNPs as shown in **Figure 3** and **Table 3**.

In previous studies, Laszlo Korosi fabricated SNPs by LAL method and concluded that size of SNPs strongly effected on the antibacterial mechanism. The antibacterial activity of SNPs

Strain	**Percentage growth inhibition of chemically synthesized SNPs**			**Percentage growth inhibition of laser-ablated SNPs**		
	(% + standard error)			**(% + standard error)**		
	Low dose (0.78μg/ml)	**Medium dose (1.57 μg/ml)**	**High dose (2.35μg/ml)**	**Low dose (0.78μg/ml_**	**Medium dose (1.57 μg/ml_**	**High dose (2.10μg/ml)**
S. aureus	41.5 ± 0.5	53.8 ± 1.7	67.02 ± 0.9	52.3 ± 0.5	76.3 ± 1.7	92.0 ± 0.9
E. coli	46.81 ± 1.7	63.2 ± 0.9	87.9 ± 0.9	57.1 ± 1.7	84.5 ± 0.9	99.81 ± 0.9
Salmonella	38.1 ± 0.3	58.9 ± 0.3	80.2 ± 0.3	40.5 ± 0.3	68 ± 0.3	82 ± 0.3
B. subtilis	31.5 ± 0.3	33.7 ± 0.3	39.9 ± 0.3	-	-	-

Table 2. Low-, medium-, and high-dose effects of laser-ablated SNPs and chemically synthesized SNPs on *S. aureus, E. coli, Salmonella,* and *B. subtilis* [57].

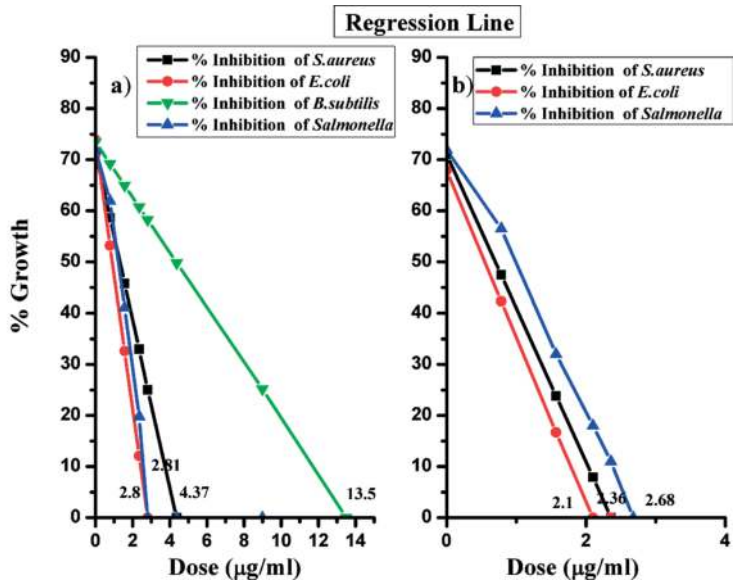

Figure 2. Regression line and percentage inhibition of *S. aureus*, *E. coli*, *B. subtilis*, and *Salmonella* by silver nanoparticles synthesized by (a) chemical and (b) laser-ablated method [57].

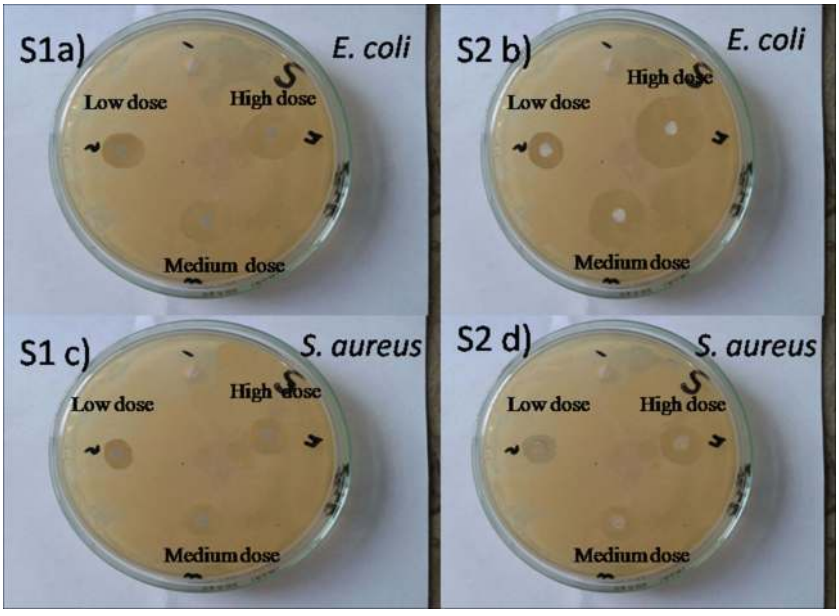

Figure 3. Well diffusion method: chemically synthesized (S1) SNPs against (a) *E. coli* and (b) *S. aureus* and laser-ablated (S2) SNPs against (c) *E. coli* and (d) *S. aureus* [57].

Strain	Zone of inhibition (mm) of chemically synthesized Ag nanoparticles (% + standard error)			Zone of inhibition (mm) of laser-ablated Ag nanoparticles (% + standard error)		
	Low dose (0.78 μg/ml)	Medium dose (1.57 μg/ml)	High dose (2.35 μg/ml)	Low dose (0.78 μg/ml)	Medium dose (1.57 μg/ml)	High dose (2.10 μg/ml)
S. aureus	11 ± 0.2	12 ± 0.3	13 ± 0.2	11 ± 0.5	13 ± 0.2	15 ± 0.3
E. coli	16 ± 1.7	19 ± 0.9	21 ± 0.9	18 ± 1.7	21 ± 0.3	23 ± 0.2

Table 3. Zone of inhibition for low, medium, and high doses of chemically synthesized and laser-ablated SNPs on *S. aureus* and *E. coli* [57].

(3 nm) was very much high against *E. coli* and SNPs (20 nm) revealed low antibacterial performance even though with concentration of 5 mg/L. However, *S. aureus* was partially with stand SNPs (3 nm) up to 5 mg/L [58]. In present study, SNPs give the best maximum zone (~ 15 and 23 mm for *S. aureus* and *E. coli*).

2.2. Antibacterial mechanism of gold nanoparticles

The antibacterial efficiency of two samples of chemically synthesized gold nanoparticles (GNPs) was evaluated by Shamaila et.al. [59]. The first sample of GNPs, G1, has a size range of ~ 6–34 nm, and the second sample, G2, has a size range ~ 20–40 nm. Their potential efficacy was checked against Gram-negative bacteria *(E. coli*, *K. pneumonia*) and Gram-positive bacteria (*S. aureus*, *B. subtilis*) by the method of turbidity and well diffusion technique [59].

2.2.1. Turbidity method

Same process was used for turbidity method as described in Section 2.1.1. Three doses were selected, low dose of ~ 1.35 μg, medium dose of ~ 2.03 μg, and High dose of 2.70 ~ μg GNPs (**Table 4**). The mean OD values with standard deviation of all test tubes for all doses were calculated carefully. The antimicrobial potential of GNPs against *S. aureus*, *K. pneumonia*, *B. subtilis*, and *E. coli* was statistically worked out. The percentage (%) declined, or enhancement in the bacterium growth was anticipated against OD value of pure (nutrient broth) media as a reference.

Observing the calculations of **Table 4**, it was concluded that GNPs of G1 sample (size range 6–34 nm) which is smaller than NPs of G2 sample revealed the reduction in percentage (%) growth. For *S. aureus*, maximum growth was calculated ~75.19% without dose [57] which declined up to 22.4%, whereas in the case of *E. coli*, maximum percentage (%) growth (74.3%) was diminished up to 6.2%. Thus, for complete percentage (%) growth inhibition for *S. aureus*, further dose will be required. For *B. subtilis*, reduction in percentage (%) growth was 45.2% only, and *K. pneumonia* was diminished up to 10%. The second set of sample G2 of GNPs with size ~ 20–40 nm intended the following behavior. *S. aureus* was reduced up to 23.7%, whereas *E. coli percentage (*%) growth decreased up to 6.2%. Percentage (%) growth reduction of *B. subtilis* was only 49.4% and percentage (%) inhibition of *K. pneumonia* was up to 13.8%.

Strain	Percentage reduction in growth of sample G1 of gold NPs (% + standard error)			Percentage reduction in growth of sample G2 of gold NPs (% + standard error)		
	Low dose (1.35μg/ml)	Medium dose (2.03 μg/ml)	High dose (2.7μg/ml)	Low dose (1.35μg/ml)	Medium dose (2.03 μg/ml)	High dose (2.7μg/ml)
S. aureus	46.4 ± 0.4	33.75 ± 1.2	22.4 ± 0.8	53.1± 0.6	40 ± 1.4	23.7 ± 0.8
E. coli	45.2 ± 1.4	26.6 ± 0.8	4.2 ± 0.8	47.6 ± 1.2	32.2 ± 0.8	6.2 ± 0.8
K. pneumonia	38.3 ± 0.4	22.8 ± 0.4	10.0 ± 0.6	42.7 ± 0.4	26.8 ± 0.4	13.8 ± 0.4
B. subtilis	57.8 ± 0.4	52.1 ± 0.6	45.2 ± 0.4	60.7 ± 0.4	56.3 ± 0.6	49.4 ± 0.4

Table 4. Antibacterial effects of two sized G1 and G2 GNPs against four bacteria [59].

The comparison of antibacterial results of two sets of samples of NPs having different sizes is given in **Table 4**. Equal doses of these samples were taken which give inhibition for each human pathogen. Sample G1 NPs exhibited more antibacterial mechanism with respect to sample G2 NPs due to size difference. There is difference in the antimicrobial results of GNPs for Gram-negative and Gram-positive bacterium. This is due to the difference in its membrane structure, i.e., the thickness of layer peptidoglycan and wide variation range between both types of bacteria [58]. Thus, inhibition of Gram-positive bacteria is achieved with higher dose of NPs.

Regression line has been plotted between doses and percentage (%) growth, exactly like silver NPs with given equations in Section 2.1.1. Curves of growth inhibition were plotted for G1 and G2 NPs. From **Figure 4**, the MIC values of sample G1 (size 7–34 nm) are calculated ~ 2.93, 3.92, 3.15, and 7.56 μg/ml for *E. coli*, *S. aureus*, *K. pneumonia*, and *B. subtilis*, respectively, whereas the MIC readings of sample G2 (size 20–40 nm) reveal 2.96, 3.98, 3.3, and 8.61 μg/ml for *E. coli*, *S. aureus*, *K. pneumonia*, and *B. subtilis*, *respectively*. A. Nanda et al. [60] observed the bactericidal potential of GNPs (40–80 nm) by agar method of diffusion and examined inhibition zone of *K. pneumonia* and *E. coli.* No noteworthy conclusions have been reported earlier for GNPs with respect to performance of SNPs [61, 62]. However, in the current project, GNPs reveal the best performance, and maximum zone was observed with dose measurement against human pathogens.

2.2.2. Well diffusion method of gold nanoparticles

The doses were further tested to examine the zone of inhibition of *S. aureus* and *E. coli* by well diffusion method. Agar plates were used to evaluate the antibacterial action of GNPs against human pathogen bacteria *E. coli* and *S. aureus*, with same method as described for SNPs. The suspension of NPs (5, 15, and 30 μl) was poured into wells named 2, 3, and 4. The inhibitory zones were measured after incubation at 37°C for 24 hours.

G1 NPs and G2 NP results from method of well diffusion against *E. coli* and *S. aureus* bacteria are given in **Figure 5** and in **Table 5**, where inhibition zones for GNPs are obvious. The inhibition zone of G1 NPs is larger than G2 NPs as confirmed (**Table 5**).

http://dx.doi.org/10.5772/intechopen.72526

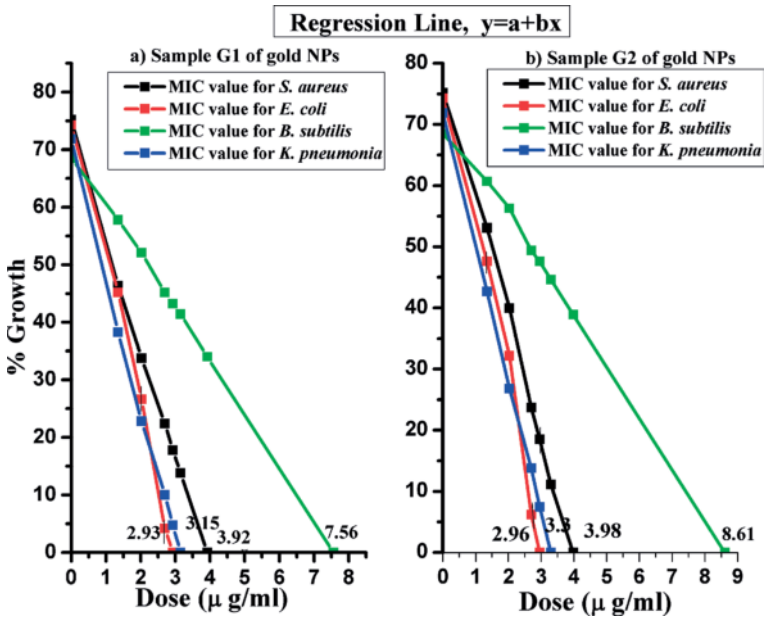

Figure 4. Calculation of doses for each bacterium: (a) sample G1 and (b) sample G2 of GNPs [59].

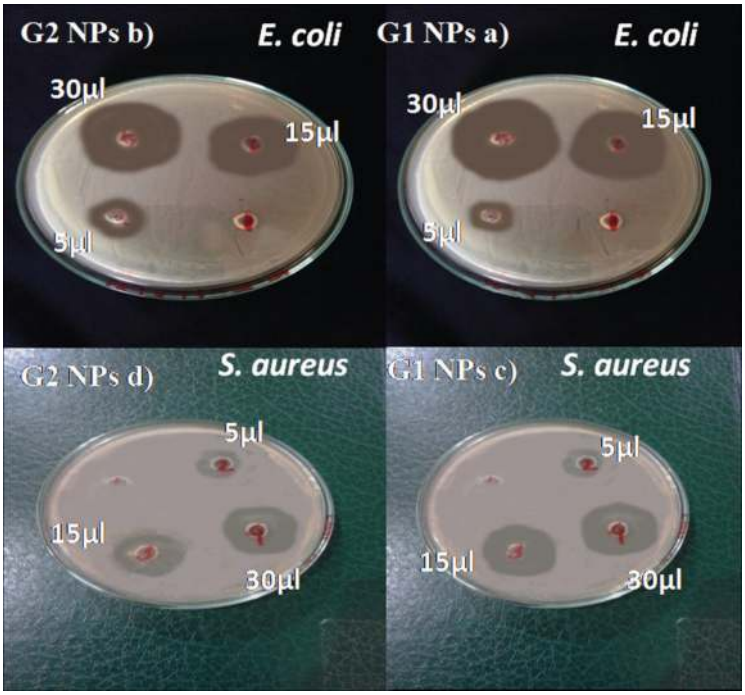

Figure 5. Well diffusion method of two sized GNPs for *E. coli* (a, b) and *S. aureus* (c, d) [59].

Micro organisms	Organism category	Dose	Zone of inhibition (mm)		
		(μL)	Control	G2 NPs	G1 NPs
S. aureus	Gram-positive	05	0	13	12
		15	0	20	23
		30	0	22	25
E. coli	Gram-negative	05	0	10	11
		15	0	28	32
		30	0	31	35

Table 5. Zone of inhibitions for samples G1 and G2 of GNPs [59].

The current research examined the calculated inhibition zone for *E. coli* which was ~ 35 mm with sample G1 and ~ 31 mm with sample G2. Similarly, the zone for *S. aureus* is ~ 25 and 22 mm with G1 and G2 samples, respectively. Previously, Nazari et al. calculated the inhibition zone ~ of 14 and 13 mm, for *E. coli* and *S. aureus* with dose of 4000 μg [63]. In present experimentation, GNPs give the best maximum zone (~ 25 and 35 mm for *S. aureus* and *E. coli*).

2.3. Antibacterial mechanism of copper nanoparticles

In the present research of Khalid et al. [64], copper nanoparticles (Cu NPs) were used to evaluate the antibacterial mechanism. The size of chemically synthesized Cu NPs without any stabilizer was rapidly increased. Antibacterial mechanism of laser-ablated Cu NPs (with filter and without filter of MCE membrane) was examined against *E. coli* and *S. aureus* by the turbidity and disk diffusion method [24].

2.3.1. Turbidity method

Three concentrations of Cu NPs were used. Cu NPs were proved to be very toxic for bacteria *E. coli* and *S. aureus*. Three factors are important in the toxicity of Cu NPs such as concentration of NPs, particle size, and bacterial growth [64, 65]. Thus, those experimental conditions were selected so that they exhibited the best curve of dose-response. Three concentrations low (1.96 μM), medium (3.92 μM), and high (5.88 μM) were prepared for Cu NPs. With these doses, the antimicrobial action of Cu NPs was observed with and without filtration of MCE by same turbidity method as described in Section 2.1.1. The MCE membrane allows the NPs to pass up to ~ 0.22 μM size. Four test tubes of each dose of Cu NPs inoculated aseptically in which one contains only control. These all test tubes were incubated for 24 h at 37°C. The percentage growth inhibitions of *S. aureus* and *E. coli* are shown in **Table 6**.

To find out how much maximum dose was required for complete reduction in the bacterial growth, statistical analysis was calculated by the equations given in Section 2.1.1. **Figure 6** represents regression line.

By chemical reduction, Cu NP doses required for maximum growth inhibition of *E. coli* calculated by regression line were 6.07 μM for with membrane and 8.33 μM for without membrane. Similarly, maximum growth inhibition for *S. aureus* was 8.32 μM with membrane and

Dose (μM)	Copper nanoparticles by chemical reduction method					
	With MCE membrane growth inhibition (%)			Without MCE membrane growth inhibition (%)		
	Low dose	Medium dose	High dose	Low dose	Medium dose	High dose
S. aureus	65.1± 0.6	48.06± 1.0	31.8± 0.8	69.6± 0.8	57.1± 1.2	42.1± 0.6
E. coli	58.3± 1.4	34.6± 0.8	1.9± 0.8	68.1± 0.6	49.8± 0.8	27.4± 1.0

Table 6. Antibacterial effects of doses of copper NPs on *E. coli* and *S. aureus*.

11.76 μM without membrane. The significant enhancement in concentration of NPs attributes higher toxicity and reduction in percentage growth of bacteria to minimum values.

2.3.2. Well diffusion method of copper nanoparticles

The zone of inhibition of laser-ablated Cu NPs was further observed [24] by agar method of well diffusion (**Table 7**). The calculations of zone of inhibition for *E. coli* and *S. aureus* are for high doses 28 ± 0.01 mm and 21 ± 0.02 mm, respectively [24]. No zone of inhibition is observed for positive control (**Figure 7**).

2.4. Antibacterial mechanism of metallic nanoparticles

Antimicrobial performance of metallic NPs depends on the features of bacterial species. The main dissimilarity between Gram-negative and Gram-positive bacteria is its membrane structure such

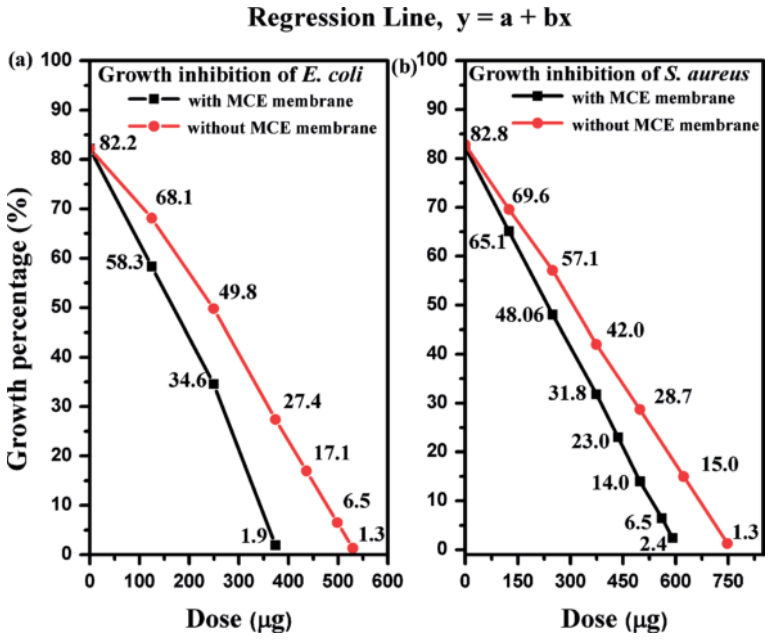

Figure 6. Graphically representation of growth inhibition by Cu NPs for (a) *E. coli* and (b) *S. aureus* estimated by regression line with and without MCE membrane.

Sr. no.	Concentration of nanoparticles	Growth of *E. coli* (%)	Growth of *S. aureus* (%)	Inhibition zone of *E. coli* (in mm)	Inhibition zone of *S. aureus* (in mm)
1	1.9 μM	52.6	60.8	16	14
2	3.9 μM	23.7	42.5	19	16
3	5.8 μM	0.9	19.3	32	-
4	6.9 μM	-	1.3	-	22

Table 7. Effects of copper NPs having low, medium, and high doses on *E. coli* and *S. aureus* [24].

that peptidoglycan layer thickness has the main features of polymer along with amino acid and sugar, thus forming an outside layer of plasma membrane (cell wall) which offers the stability to structure which is responding to the osmotic pressure of cytoplasm. Its range of thickness is higher (50%) in Gram-positive (+) and lower (8%) in Gram-negative (−) bacterium. Gram-positive bacterium comprises peptidoglycan layer in multiple steps having long teichoic acid chain. Conversely, Gram-negative bacteria contain a single and thin peptidoglycan layer with the absence of teichoic acid. Outer membrane has periplasmic and lipopolysaccharide layer [58].

Thus, the main process is first the attachment of metal ions or NPs to the bacterium outer cell wall and then accumulation of protein precursor's layer, which ultimately disables the proton motive force. Metallic NP destabilizes the outer membrane, produces crack in the membrane of plasma, and reduces the synthase activities of the depletion layer of intracellular adenosine triphosphate (ATP) [31], thus reducing the process of metabolism. It destructs the ribosome subunit by t RNA binding and thus finally the total collapse of biological mechanism.

It has been further concluded that the small-sized metallic NPs with larger surface area exhibited some electronic effects which were beneficial to improve the surface attraction of NPs. In addition, the percentage of enhanced surface area straightly interacted with the membrane of microorganism with vast extent and hence bridged an improved relation with bacteria. These two vital factors powerfully enhanced the antimicrobial action of the NPs with high surface

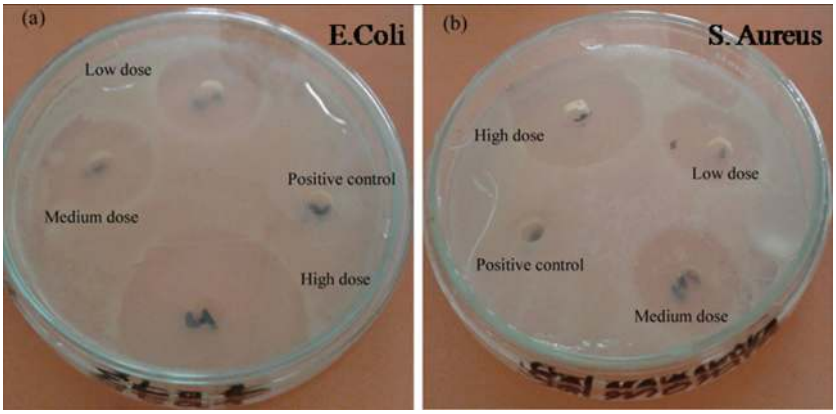

Figure 7. Zone of inhibition by Cu NPs in mm for (a) *E. coli* and (b) *S. aureus* [24].

area. Bacterial proteins (cell wall and cytoplasm) were accountable for the cell performance. These NPs disrupted the normal performance of protein function, which causes the cell's death. NPs basically interacted with soft bases having sulfur or phosphorus components. So, the sulfur of proteins and phosphorus belonging to DNA molecules are favorite attacking sites of NPs. Then, these NPs attached themselves to enzymes (thiol groups), i.e., nicotinamide adenine dinucleotide (NADH) dehydrogenases and destructed its respiratory chain by releasing of oxygen species, thus creating oxidative stress. Consequently, a major damage is occurred in the cell structures and lastly leads to cell loss [21, 59].

Shrivastava et al. [66] have reported that the SNPs affected *S. aureus* in lesser amount. The bacterium *B. subtilis* has been considered a most powerful bacterium (Gram-positive). The reason is that it can stay alive easily in any rigid condition due to endospore formation (stress-resistant) and its formation of DNA externally which can be produced by recombination with original DNA at its last stage and can tolerate under adverse situations. *Salmonella* also exhibits more resistance with respect to *E. coli*.

In the present research work, SNPs exhibited effective antibacterial behavior against *E. coli* bacterium with respect to other bacterium. *S. aureus* exhibited more resistance than *E. coli*; so, selected dose (high ~2.10 μg/ml) is quite enough for maximum inhibition of *E. coli*. Due to variation in peptidoglycan layer in Gram-positive bacteria, more doses of SNPs would be recommended for full inhibition of *Salmonella* and *S. aureus*. The laser-ablated SNPs have demonstrated and elevated antibacterial behavior due to small size and purity of NPs which may be beneficial in wood flooring, coatings, and cotton textile industries.

It is demonstrated that the small-sized GNP sample ~ 6–34 nm displays good bacterial performance than the second GNP sample ~ 20–40 nm. This advantage is by reason of its minute size, enhanced surface-area-to-volume ratio, and fine penetration power. Finally, the small-sized NPs effortlessly bind to the prominent parts of the outer membrane, so causing damages in structure, deprivation, and ultimately cell death. Various GNP doses displayed the best antibacterial action against *E. coli* with respect to other tested bacteria. Similarly, dose of 2.70 μg/ml was quite sufficient for *K. pneumonia* and for *E. coli's* complete inhibition. More NP doses were recommended for total inhibition of *S. aureus* and *B. subtilis* because of their difference of peptidoglycan layer. Here, *B. subtilis* had been considered the most resistive Gram-positive bacteria in the performed experimentation.

It is evident that for both Gram-positive and Gram-negative bacteria, the increase in the concentration of Cu NPs revealed the decrease in percentage growth. With high dose of Cu NPs, a noticeable antibacterial action (growth inhibition ~ 1.9%) was recorded for *E. coli* with filtered NPs (smaller in size); however, at the same time for nonfiltered dose (larger in size), the percentage growth decreases up to only 27%. Similarly, the percentage growth of *S. aureus* for filtered NPs decreased up to 31.8% and for non-filtered up to ~ 42.1% only. The clear difference in percentage (%) growth inhibition for both strains of bacteria was deeply attributed to the concentration of NPs and size of NPs. These outcomes concluded that the further doses of Cu NPs are required to show full antibacterial action against these bacterial strains. The cell wall of Gram-positive bacteria is composed of heavy layer of peptidoglycan (about ~ 20–80 nm), forming a three-dimensional structure of rigid tissues. This rigidity protects the cell wall, provides only fewer sites for Cu NPs, and does not allow to penetrate the NPs [24].

In current research, the observed antibacterial mechanism of all metallic NPs is tested on behalf of concentration and size of NPs. The basic mechanism is that how many metal ions are released because they attributed to their large surface-area-to-volume ratio. These ions directly interact with each bacterium's outer membrane. One possible justification is nanometer size pores of bacteria cell membranes that can give a pathway for the NPs [59]; secondly, the ions released by NPs may fasten to the cell wall of bacteria and crack it. Ions of NPs which are released produce radicals of hydroxyl that may deform the basic function of essential proteins and finally its DNA for the cell death [57–59].

3. Conclusion

The two techniques for fabricating metallic nanoparticles were compared here to specify a broad range of achievable characteristics. This aptitude to give variation in properties of controllable metallic nanoparticles would be eventually profitable for future research relaying on the antibacterial properties of nanoparticles. A direct assessment between metallic NPs generated either by wet chemical technique or LAL method will be supportive in finding the exact trends and mechanisms of antimicrobial, which are currently hot issues of recent advance research. The antibacterial activity was size and dose dependent and was more explicit against Gram-negative bacterium than Gram-positive ones. The fabricated nanoparticles are spherical in shape with polycrystalline nature having various size ranges in nm. Antibacterial behavior of metallic nanoparticles against pathogenic bacteria demonstrates that they can act as an efficient tool for antibacterial. Silver, gold, and copper nanoparticles exhibit their excellent performance physically, catalytically, and chemically because of its larger surface-area-to-volume ratio. Turbidity provides an efficient and fast technique for the estimation of the bacterial development in a liquid. The calculations of MIC are further supportive in calculation of inhibition zone by agar method of diffusion. The present study will be beneficial in environment, information technology, health, cosmetics, and food department fields. Additionally, silver nanoparticles have reduced the life-threatening facts because of their flexible nature with respect to conventional antibiotics. Gold nanoparticles provide benefit in the field of biomedicine, chemistry, and genetics due to their characteristics of functionally active power. In biomedicine, gold NPs can become a vital revolution in the research of drug delivery and cancer therapy. They also proved to be nontoxic and a safe antimicrobial representative due to their powerful functional nature instead of antibiotics. Antimicrobial nanomaterials are potentially eye-catching for a variety of medical applications, i.e., dental procedures. Copper nanoparticles perform best as an antibiotic, antifungal, and antimicrobial agent when utilized for plastics, textiles, and coatings. Copper and its oxide are used for the coating of cellulose of nanofibrillar, a promising nanobiomaterial. The metallic nanoparticles showed potential performance as an antimicrobial against *E. coli*, *S. aureus*, *B. subtilis*, and *Salmonella* and are suggested as an alternative antibacterial nanobiotics.

Acknowledgements

We are highly thankful to Microbiology Department of the University of Veterinary and Animal Sciences, Lahore, Pakistan, for providing facilities for antibacterial analysis. Furthermore,

appreciation is given to the assistance of the Physics Department, University of Engineering and Technology, Lahore, Pakistan. Authors are highly obliged to the editors of Intech Open Book for providing this great opportunity.

Author details

Shamaila Shahzadi*, Nosheen Zafar and Rehana Sharif

*Address all correspondence to: drshamaila.uet@gmail.com

University of Engineering and Technology, Lahore, Pakistan

References

[1] Popa M, Pradell T, Crespo D, Calder´on-Moreno JM. Stable silver colloidal dispersions using short chain polyethylene glycol. Colloids and Surfaces A: Physicochemical and Engineering Aspects. 2007;**303**:184-190

[2] Abdel Halim MAK, Mady MM, Ghannam MM. Physical properties of different gold nanoparticles: Ultraviolet-visible and fluorescence measurements. Journal of Nanomedicine and Nanotechnology. 2012;**3**:3

[3] Amendola V, Meneghetti M. Size evaluation of gold nanoparticles by UV-vis spectroscopy. Journal of Physical Chemistry C. 2009;**113**:4277-4285

[4] Abkhoo J, Panjehkeh N. Evaluation of antifungal activity of silver nanoparticles on *Fusarium oxysporum*. International Journal of Infection. In press (In press): 2016;e41126. Doi: 10.17795/iji-41126

[5] Tolaymat TM, El BAM, Genaidy A, Scheckel KG, Luxton TP, Suidan M. An evidence-based environmental perspective of manufactured silver nanoparticle in syntheses and applications: A systematic review and critical appraisal of peer-reviewed scientific papers. Science of the Total Environment. 2010;**408**(5):999-1006. DOI: 10.1016/j.scitotenv.2009. 11.003

[6] Prabhu S, Poulose EK. Silver nanoparticles. Mechanism of antimicrobial action, synthesis, medical applications, and toxicity effects. International Nano Letters. 2012;**2**:32

[7] Giasuddin ASM, Jhuma KA, MujibulHaqA M. Use of gold nanoparticles in diagnostics, surgery and medicine: A review. Bangladesh Journal of Medicine and Biochemistry. 2012;**5**(2):56-60

[8] Jain S, Hirst DG, O'Sullivan JM. Gold nanoparticles as novel agents for cancer Therapy. The British Journal of Radiology. 2012;**85**:101-113

[9] Misbahi A. A review on gold nanoparticles radio sensitization effect in radiation therapy of cancer. Reports of practical oncology and radiotherapy. 2010;**15**:176-180

[10] Yugang SUN, Changhua AN. Shaped gold and silver nanoparticles. Frontier of Material Science. 2011;**5**(1):1-24

[11] Zhang Z, Ross RD, Roeder RK. Preparation of functionalized gold nanoparticles as a targeted X-ray contrast agent for damaged bone tissue. Nanoscale. 2010;**2**:582-586

[12] Capek I. Preparation, functionalization of gold nanoparticles. Journal of Surface Science & Technology. 2013;**29**(3-4):1-18

[13] Coradeghini R, Gioria S, García CP, Nativo P, Franchini F, Gillil D, Ponti J, Rossi F. Size-dependent toxicity and cell interaction mechanisms of Gold nanoparticles on mouse fibroblasts. Toxicology Letter. 2013;**217**:205-216

[14] Tan KS, Cheong KY. Advances of Ag, Cu, Ag–Cu alloy nanoparticles synthesized via chemical reduction route. Journal of Nanoparticle Research. 2013;**15**:1537. DOI: 10.1007/s11051-013-1537-1

[15] Galletti AMR, Antonetti C, Marracci M, Piccinelli F, Tellini B. Novel microwave-synthesis of Cu nanoparticles in the absence of any stabilizing agent and their antibacterial and antistatic applications. Applied Surface Science. 2013;**280**:610-618

[16] Grace AN, Pandian K. Antibacterial efficacy of amino glycosidic antibiotics protected gold nanoparticles—A brief study. Colloids and Surfaces A: Physicochemical and Engineering Aspects. 2007;**297**:63-70

[17] Naika HR et al. Green synthesis of CuO nanoparticles using *Gloriosa superba* L. extract and their antibacterial activity. Journal of Taibah University of Science. 2014;**9**:7-12

[18] Punnoose A, Dodge K, Rasmussen JW, Chess J, Wingett D, Anders C. Cytotoxicity of ZnO nanoparticles can be tailored by modifying their surface structure: A green chemistry approach for safer nanomaterials. ACS Sustainable Chemistry & Engineering. 2014;**2**:1666-1673

[19] Nadagouda MN, Iyanna N, Lalley J, Han C, Dionysiou DD, Varma RS. Synthesis of silver and gold nanoparticles using antioxidants from blackberry, blueberry, pomegranate, and turmeric extracts. ACS Sustainable Chemistry & Engineering. 2014;**2**:1717-1723

[20] Amendola V, Meneghetti M. What controls the composition and the structure of nanomaterials generated by laser ablation in liquid solution. Physical Chemistry Chemical Physics. 2013;**51**:3027-3046

[21] Zeng H, Du X-W, Singh SC, Kulinich SA, Yang S, He J, Cai W. Nanomaterials via laser ablation/irradiation in liquid: A review. Advance Functional Materials. 2012;**22**:1333-1353

[22] Rao SV, Podagatlapalli GK, Hamad S. Ultrafast laser ablation in liquids for nanomaterials and applications. Journal of Nanoscience and Nanotechnology. 2014;**14**:1364-1388

[23] Naddeo JJ, Ratti M, O'Malley SM, Griepenburg JC, Bubb DM, Klein EA. Antibacterial properties of nanoparticles: A comparative review of chemically synthesized and laser-generated particles. Advanced Science, Engineering and Medicine. 2015;**7**(12):1044-1057

[24] Khalid H, Shamaila S, Zafar N, Sharif R, Nazir J, Rafique M, Ghani S, Saba H. Antibacterial behavior of laser-ablated copper nanoparticles. Acta MetallurgicaSinica (English Letters). 2016;**29**(8):748-754. DOI: 10.1007/s40195-016-0450-x

[25] Debanath MK, Karmakar S. Study of blueshift of optical band gap in zinc oxide (ZnO) nanoparticles prepared by low-temperature wet chemical method. Material Letters. 2013;**111**:116-119

[26] Turkevich J, Stevenson PC, Hillier J. A study of the nucleation and growth processes in the synthesis of colloidal gold. Discussion of Faraday Society. 1951;**11**:55-75

[27] Swain B, Hong HS, Jung HC. Commercial process development for synthesis of spherical cobalt nanopowder by wet chemical reduction reaction. Chemical Engineering Journal. 2015;**264**:654-663

[28] Lu K, Zhao J. Equiaxed zinc oxide nanoparticle synthesis. Chemical Engineering Journal. 2010;**160**:788-793

[29] Ethiraj AS, Kang DJ. Synthesis and characterization of CuO nanowires by: A simple wet chemical method. Nanoscale Research Letter. 2012;**7**(1):70

[30] Zeng J, Zhu C, Tao J, Jin M, Zhang H, Li ZY, Zhu Y, Xia Y. Controlling the nucleation and growth of silver on palladium nanocubes by manipulating the reaction kinetics. AngewandteChemie International Edition. 2012;**51**:2354-2358

[31] ThanhN TK, MacleanN MS. Mechanisms of nucleation and growth of nanoparticles in solution. Chemical Reviews. 2014;**114**(15):7610-7630. DOI: 10.1021/cr400544s

[32] Schladt TD, Schneider K, Schild H, Tremel W. Synthesis and bio-functionalization of magnetic nanoparticles for medical diagnosis and treatment. Dalton Transaction. 2011;**40**:6315-6343

[33] Perala SRK, Kumar S. On the mechanism of metal nanoparticle synthesis in the Brust–Schiffrin method. Langmuir. 2013;**29**:9863-9873

[34] Niu W, Zhang L, Xu G. Seed-mediated growth of noble metal nanocrystals: crystal growth and shape control. Nanoscale. 2013;**5**:3172-3181

[35] Xia Y, Xia X, Wang Y, Xie S. Shape-controlled synthesis of metal nanocrystals. MRS Bulletin. 2013;**38**:335-344

[36] Ivask A et al. Toxicity mechanisms in *Escherichia coli* vary for silver nanoparticles and differ from ionic silver. ACS Nano. 2014;**8**:374-386

[37] Alexander JW. History of the medical use of silver. Surgical Infections (Larchmt). 2009;**10**:289-292

[38] Grass G, Rensing C, Solioz M. Metallic copper as an antimicrobial surface. Applied and Environmental Microbiology. 2011;**77**:1541-1548

[39] Ruparelia JP, Chatterjee A, Duttagupta SP, Mukherji S. Strain specificity in antimicrobial activity of silver and copper nanoparticles. Acta Biomaterialia. 2008;**4**:707-716

[40] Dizaj SM, Lotfipour F, Barzegar-Jalali M, Zarrintan MH, Adibkia K. Antimicrobial activity of the metals and metal oxide nanoparticles. Materials Science and Engineering C. 2014;**44**:278-284

[41] Zhang L, Jiang Y, Ding Y, Daskalakis N, Jeuken L, Povey M, O'Neill AJ, York DW. Mechanistic investigation into antibacterial behaviour of suspensions of ZnO nanoparticles against *E. coli*. Journal of Nanoparticle Research. 2010;**12**:1625-1636

[42] Pelgrift RY, Friedman AJ. Nanotechnology as a therapeutic tool to combat microbial resistance. Advance Drug Delivery Review. 2013;**65**:1803-1815

[43] Arias CA, Murray BE. A new antibiotic and the evolution of resistance. The New English. Journal of Medicine. 2015;**372**:1168-1170

[44] Ivask A, Kurvet I, Kasemets K, Blinova I, Aruoja V, Suppi S, Vija H, Ka¨kinen A, Titma T, Heinlaan M, Visnapuu M, Koller D, Kisand V, Kahru A. Size-dependent toxicity of silver nanoparticles to bacteria, yeast, algae, crustaceans and mammalian cells in vitro. PLOS One. 2014;**9**(7):e102108

[45] Guzman M, Dille J, Godet S. Synthesis and antibacterial activity of silver nanoparticles against Gram-positive and Gram-negative bacteria. Nanomedicine Nanotechnology, Biology Medicine. 2012;**8**:37-45

[46] Azam A, Ahmed AS, Oves M, Khan MS, Memic A. Size-dependent antimicrobial properties of CuO nanoparticles against Gram-positive and -negative bacterial strains. International Journal of Nanomedicine. 2012;**7**:3527-3535

[47] Kim TH, Kim M, Park HS, Shin US, Gong MS, Kim HW. Size-dependent cellular toxicity of silver nanoparticles. Journal of Biomedical Material Research-Part A. 2012;**100 A**: 1033-1045

[48] Raghupathi KR, Koodali RT, Manna AC. Size-dependent bacterial growth inhibition and mechanism of antibacterial activity of zinc oxide nanoparticles. Langmuir. 2011;**27**:4020-4028

[49] You C, Han C, Wang X, Zheng Y, Li Q, Hu X, Sun H. The progress of silver nanoparticles in the antibacterial mechanism, clinical application and cytotoxicity. Molecular Biology Reports. 2012;**39**:9193-9201

[50] Dutta RK, Nenavathu BP, Gangishetty MK, Reddy AVR. Studies on antibacterial activity of ZnO nanoparticles by ROS induced lipid peroxidation. Colloids Surfaces B Bio interfaces. 2012;**94**:143-150

[51] Raffi M, Hussain F, Bhatti TM, Akhter JI, Hameed A, Hasan MM. Antibacterial characterization of silver nanoparticles against *E. coli* ATCC-15224. Journal of Material Science and Technology. 2008;**24**:192-196

[52] Baek YW, An YJ. Microbial toxicity of metal oxide nanoparticles (CuO, NiO, ZnO, and Sb_2O_3) to *Escherichia coli*, *Bacillus subtilis*, and *Streptococcus aureus*. Science of the Total Environment. 2011;**409**:1603-1608

[53] Jung WK, Koo HC, Kim KW, Shin S, Kim SH, Park YH. Antibacterial activity and mechanism of action of the silver ion in *Staphylococcus aureus* and *Escherichia coli*. Applied of Environmental Microbiology. 2008;**74**(7):2171-2178. DOI: 10.1128/AEM.02001-07

[54] Madigan MT, Martinko JM, Stahl DA, Clark DP. Brock Biology of Microorganisms, 13th Ed. San Francisco, CA: Pearson Prentice Hall Inc; 2006. 129-130 pp

[55] Ben-David A, Davidson CE. Estimation method for serial dilution experiments. Journal of Microbiological Methods. 2014;**107**:214-221

[56] Pommerville JC. Alcamo's Fundamentals of Microbiology. 9th Ed. Canada: Jones and Bartlett Publishers; LLC. 2011. 105 pp

[57] Zafar N, Shamaila S, Nazir J, Sharif R, Rafique MS, Hasan J, Ammara S, Khalid H. Antibacterial action of chemically synthesized and laser generated silver nanoparticles against human pathogenic bacteria. Journal of Material Science and Technology. 2016;**32**(8):721-728. DOI: 10.1016/j.jmst.2016.05.009

[58] Kyrösi L, Rodio M, Dömötör D, Kovács T, Papp S, Diaspro A, Intartaglia R, Beke S. Ultrasmall, ligand-free Ag nanoparticles with high antibacterial activity prepared by pulsed laser ablation in liquid. Hindawi Publishing Corporation Journal of Chemistry. 2016;**2016**:Article ID 4143560. 8 pages. http://dx.doi.org/10.1155/2016/4143560

[59] Shamaila S, Zafar N, Riaz S, Sharif R, Nazir J, Naseem S. Gold nanoparticles: An efficient antimicrobial agent against enteric bacterial human pathogen. Nanomaterials. 2016;**6**:71. DOI: 10.3390/nano6040071

[60] Belliraj TS, Nanda A, Ragunathan R. In-vitro hepatoprotective activity of *Moringa oleifera* mediated synthesis of Gold nanoparticles. Journal of Chemical and Pharmaceutical Research. 2015;**7**:781-788

[61] Chatterjee S, Yopadhyay AB, Sarkar K. Effect of iron oxide and Gold nanoparticles on bacterial growth leading towards biological application. Journal of Nanobiotechnology. 2011;**9**:34. DOI: 10.1186/1477-3155-9-34

[62] Badwaik VD, Vangala LM, Pender DS, Willis CB, Aguilar ZP, Gonzalez MS, Paripelly R, Dakshinamurthy R. Size-dependent antimicrobial properties of sugar-encapsulated gold nanoparticles synthesized by a green method. Nanoscale Research Letters. 2012;**7**:623. DOI: 10.1186/1556-276X-7-623

[63] Nazari ZE, Banoee M, Sepahi AA, Rafii F, Shahverdi AR. The combination effects of trivalent gold ions and gold nanoparticles with different antibiotics against resistant Pseudomonas aeruginosa. Gold Bulletin. 2012;**45**:53-59

[64] Khalid H, Shamaila S, Zafar N. Synthesis of copper nanoparticles by chemical reduction method. Scientific International (Lahore). 2015;**27**(4):3085-3088. ISSN 1013-5316; CODEN: SINTE 8

[65] Selvarani M, Prema P. Evaluation of antibacterial efficacy of chemically synthesized copper and zero valent iron nanoparticles. Asian Journal of Pharmaceutical and Clinical Research. 2013;**6**(3):223-227

[66] Shrivastava S, Bera T, Roy A, Singh G, Ramachandrara P, Dash D. Characterization of enhanced antibacterial effects of novel silver nanoparticles. Nanotechnology. 2007;**18**: 225103 (9pp)